Astron. Astrophys. 318, 289–292 (1997)

ASTRONOMY AND ASTROPHYSICS

Research Note

Evolution of force-free electric currents in the solar atmosphere

M. Karlický

Astronomical Institute of the Academy of Sciences of Czech Republic, CZ-251 65 Ondřejov, Czech Republic

Received 6 May 1996 / Accepted 25 June 1996

Abstract. The new 3-D numerical model studying evolution of force-free electric currents in the solar atmosphere is presented. The initial dipole magnetic field is considered in a simplified active region. Starting from a low electric current, which penetrates the photosphere, and increasing the current intensity, the path of force-free electric current and the corresponding magnetic field are computed. The virtual mirror current representing the effect of the inertial photosphere is considered. The single and the multiple current paths are compared. For the single path case, it was found that an arch-shape electric current is sheared with the increasing current intensity, then screwed into a current loop with the helical structure and when the electric current generates a magnetic field greater than the initial dipole magnetic field the current path becomes unstable. During all this process the current path moves upwards. Although the multiple current paths show more complex internal structures of electric currents, the global aspect of these processes remains the same. The relevance of this modelling for processes in the solar atmosphere is discussed.

Key words: MHD – Sun: activity – magnetic fields

1. Introduction

It is commonly believed that electric currents flow in the solar atmosphere and form electric circuits between subphotospheric and coronal layers (Alfvén and Carlqvist, 1967; Alfvén, 1977; Spicer, 1982; Melrose, 1995). Measurements of the photospheric vector magnetic field show positions where the currents cross the photosphere (de La Beaujardière et al., 1993; Hofmann, 1995). The measured total current and current density are in the range of 10^{11} - 10^{12} A and 10^{-3} - 10^{-2} A m^{-2}, respectively (Hagyard, 1988). It is expected that the electric currents are flowing in so called quasi-separatrix layers (Démoulin et al., 1996). These currents and the corresponding magnetic fields represent the free energy which can be released during solar flares. The magnetic field reconnection and coalescence of electric currents are considered as the mechanisms releasing this energy (Priest, 1994; Tajima et al., 1987). Thus, electric currents play an important role in the solar flare theory as well as in the theory of pre-flare filaments. It was suggested by Van Tend and Kuperus (1978) that the filament can be destabilized by an increase of the electric current flowing in this filament. This idea was generalized by Kaastra (1985), Martens (1986), and by Forbes and Isenberg (1991) who presented models of solar flares. But the question arises: What are the real paths of electric currents in the solar atmosphere and how to determine these paths?

In the following, we first present a new model computing this electric current path and then we use this model for the single and multiple current paths cases.

2. Numerical model

A basic assumption in this model is that the electric current is force-free, i.e. the electric current is parallel to the local magnetic field. The currents are represented by numerical particles (6400 in our case). First some initial magnetic field of arbitrary form (potential or force-free) is prescribed. Then from the bottom surface of the numerical box, which represents the photosphere, numerical particles (no mass, no forces, no equation of motion are considered) are injected upwards along the local magnetic field line. These particles change their position with the constant "velocity" $\mathbf{v} \parallel \mathbf{B}$ ($\mathbf{B}$ is the magnetic field) throughout the space above the photosphere. During the "time" step Δt, they change their position by the propagation vector $\mathrm{d}\mathbf{l} = \mathbf{v}\Delta t$, which simultaneously represents the force-free electric current, whose intensity is prescribed by a numerical constant. Because the particles are injected successively, one particle every time step Δt along one current path, they are after some time distributed regularly (with the $\mathrm{d}\mathbf{l}$ distance between neighbouring particles) along a line above the photosphere, thus depicting the electric current path. For small currents these paths correspond to the initial magnetic field lines. If particles penetrate back below the photosphere then these particles are excluded from

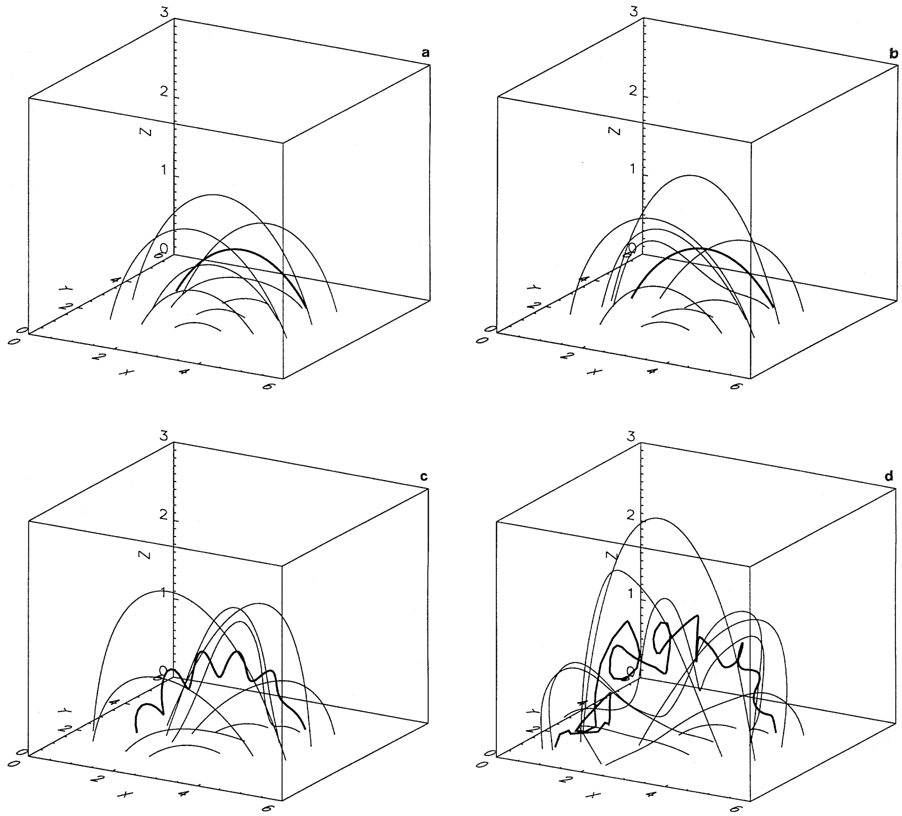

Fig. 1a–d. The single electric current path (thick line) and magnetic field (thin lines) for I = 5×10^{10} A **a**, I = 1×10^{11} A **b**, I = 2×10^{11} A **c**, and 3×10^{11} A **d**. The distances are expressed in 10^4 km.

further computations. Prescribing to each particle some electric current and using the Biot and Savart law

$$d\mathbf{B} = \mu_0 I \frac{d\mathbf{l} \times \mathbf{R}}{4\pi \mid \mathbf{R} \mid^3}, \tag{1}$$

where **R** is the distance from the current element to where d**B** is evaluated and d**l** is the element of length in the current direction (which, in our case, is equal to the particle propagation vector - see above), we compute the current magnetic field, which changes the initial magnetic field as well as the current particle trajectories. Namely, at every time step, at particle positions we compute the magnetic field directions, which are then used as directions of the particle propagation. This procedure is repeated every time step. At some specific times the magnetic field is also available at any point of the computational box, e.g. for field-line drawings. The relation (1) is singular for $\mid \mathbf{R} \mid = 0$. Moreover, the electric current is flowing in some finite area. On the other hand, there is the finite distance between numerical particles. To solve this problem, we define $\mathbf{R_0}$ as the minimum interaction distance; while for the magnetic field calculations at distances $\mid \mathbf{R} \mid > \mid \mathbf{R_0} \mid$ the relation (1) is valid, for the case $\mid \mathbf{R} \mid \leq \mid \mathbf{R_0} \mid$ a modified relation in the form

$$d\mathbf{B} = \mu_0 I \frac{d\mathbf{l} \times \mathbf{R}}{4\pi \mid \mathbf{R_0} \mid^3} \tag{2}$$

is used (in this relation $d\mathbf{B}$ decreases to zero for $\mid \mathbf{R} \mid \rightarrow 0$). Thus $\mid \mathbf{R_0} \mid$ roughly corresponds to the radius of the electric current cross-section. (In principle, Eq. (2) can be replaced by some cylindrical or other approximation. But we think that these changes cause only slight effects on global equilibria. The reason why Eq. (2) was used is the simplicity of its numerical form, which is important in the case with many numerical particles.) Simultaneously, this procedure represents some smoothing of electric current. Namely, in the force-free case, the curved, infinitesimally thin electric current always forms a helical structure. This effect is also found for smoothed electric currents, but with much larger structures. To describe this helical structure with the appropriate precision, we need the smoothing distance $\mathbf{R_0}$ to be several times greater than the distance between successively injected particles. Otherwise, we have more helical circles, which are not sufficiently described by particles. This smoothing procedure is a little artificial and can be considered as appropriate only if we are interested in the global aspects of electric current and magnetic field. More precise computations can be done only if one localized electric current is represented by many close current paths. When the minimum interaction distance $\mathbf{R_0}$ is shorter than the distances between numerical particles d**l**, then the procedure with $\mathbf{R_0}$ becomes irrelevant and the smoothing of currents is given by d**l**. More precision can be obtained only by the shortening of d**l**. Therefore, according to the type of our task, we need to select the appropriate d**l**, $\mathbf{R_0}$, number of current paths and number of particles.

Our computations start from a low electric current which is then slowly and continuously increased to the specific value of electric current. Then it is useful to keep constant this current for some time and thus to relax the resulting structure. The method can be generalized for an arbitrary number of injec-

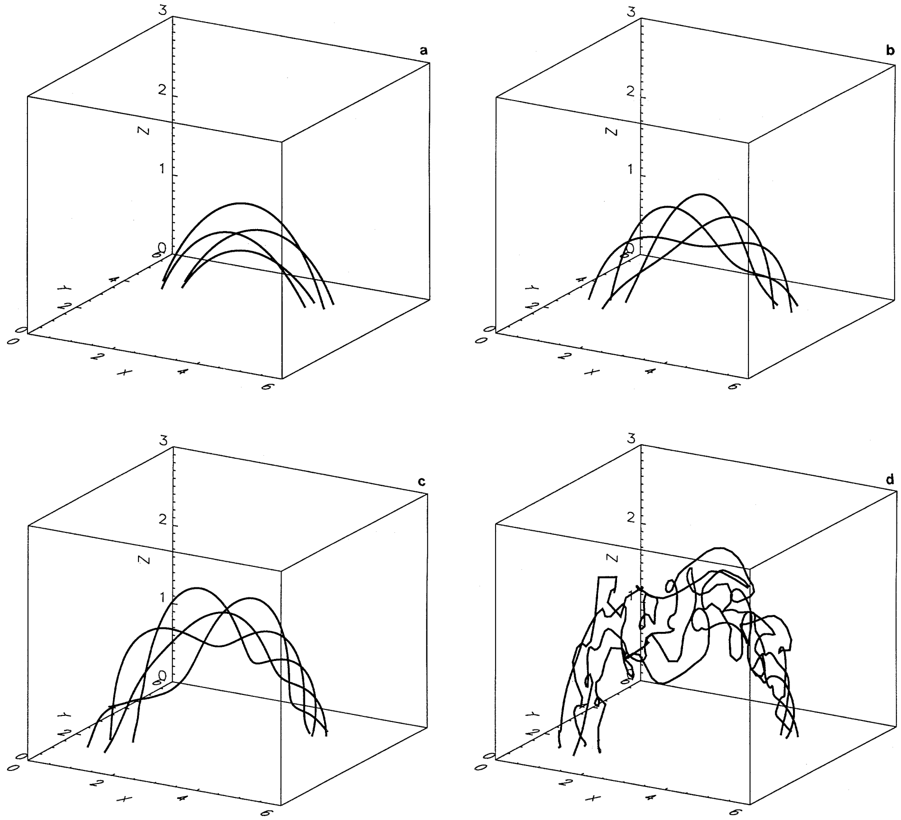

Fig. 2a–d. The four electric current paths for $I_{total} = 5 \times 10^{10}$ A **a**, $I_{total} = 2 \times 10^{11}$ A **b**, $I_{total} = 3 \times 10^{11}$ A **c**, and 3.5×10^{11} A **d**. The distances are expressed in 10^4 km.

tion positions, i.e. for arbitrary current distribution. It enables us, for example, to simulate the current flowing through a finite cross-section by more sub-currents and thus to increase the computation precision.

Applying this method to currents in the solar atmosphere we need to consider the effect of the inertial photosphere. We included this effect using the virtual mirror current as suggested by Kuperus and Raadu (1974). This current causes that no magnetic field created by the coronal currents can penetrate the photospheric layers. This procedure is in agreement with the specification of the boundary condition at the photospheric layer (see Sakurai, 1981).

3. Results of numerical modelling

As the initial magnetic field of a simplified active region (i.e. without computed currents), we take the dipole magnetic field:

$$B_x = C\frac{3x^2 - r^2}{r^5}, \tag{3}$$

$$B_y = C\frac{3xy}{r^5}, \tag{4}$$

$$B_z = C\frac{3x(z - z_0)}{r^5}, \tag{5}$$

where C is a constant, z_0 is the position of the magnetic source below the photosphere (z_0 = - 5 $\times$ 10^7 m in our case), r is the distance from the magnetic source position to the position where the magnetic field is calculated. The constant C is chosen to give the maximum of this field as 100 G. This maximum is situated in the bottom-surface centre of the computational box. Then using our model with the increasing electric current we computed force-free current paths for two cases: a) the current is represented by a single current path with $| \mathbf{R_0} | = 4 \times 10^6$ m, and b) the current is represented by four current paths having the distances of 4×10^6 m at injection positions with $| \mathbf{R_0} | = 2 \times 10^6$ m. It means that in both cases the current cross-section area is 5×10^{13} m^2. The distance between particles is 5×10^5 m, the particle "velocity" is 5×10^5 m s^{-1}, and the "time" step is 1 s. The results for a single current path with the electric currents: 5×10^{10}, 1×10^{11}, 2×10^{11}, and 3×10^{11} A are shown in Fig. 1. In computations the electric current was increased up to a specific value and then kept constant for some relaxation time. The corresponding magnetic field is included for an illustration. You can see strong deviations from the initial magnetic field. On the other hand, results with four current paths for total electric currents: 5×10^{10}, 2×10^{11}, 3×10^{11}, and 3.5×10^{11} A are depicted in Fig. 2.

In both cases, for low electric currents the current path is close to the dipole magnetic field line (Fig. 1a), while for higher currents the current path becomes sheared (Fig. 1b) and then the current path is screwed into the helical structure (Fig. 1c). Simultaneously with the current increase the current paths move upwards (Fig. 1 and 2).

We studied the stability of computed structures. It was found that the configurations in Figs. 1a, 1b, and 2a, 2b, are quite stable in time. As concerns Figs. 1c and 2c, the global arch is stable, the helical structure keeps its form, but it shows some oscillatory motion along the arch axis. On the other hand, those in Figs. 1d and 2d are unstable, their internal structure is strongly variable, the global shape shows some stability, distances between the particles do not remain the same, i.e. the correct description of the electric current is disturbed. It seems that there is some critical electric current, above which no force-free electric current structures exist.

Comparing the single current path case with that of four paths, we can see that the global features remain the same. It can also be seen that the stability of the current paths is better in the four path case in comparison with the single path case.

4. Discussions and conclusions

In this paper, starting from a low electric current in the dipole magnetic field we computed the force-free current path and magnetic field for currents from 0 to 3.5×10^{11} A. More stable results were obtained when the electric current was represented by more current paths.

We found the shearing and uprising of electric currents. Simultaneously, the surrounding magnetic field was deformed. Moreover, the individual electric current forms a helical structure, which can be searched in observations. Evidently all these features are important for the active region evolution, filament formation and disruption, eruptive prominences, coronal mass ejections and solar flares.

It seems that there is some critical electric current, above which no force-free electric current structures exist. This aspect is interesting from the point of view of mass ejection, but clearly, it needs further verifications.

In our computations we used the constant $\mathbf{R_0}$ along the current path. This simplification can be supported by the observation of loops with nearly constant thickness (Klimchuk et al., 1992). Otherwise, $\mathbf{R_0}$ needs to depend on the magnetic field.

The present method of current path computations can be used not only for the initially potential magnetic field, but also for the linear force-free magnetic field. In this case the computed currents are considered as additional currents to initial current densities.

The presented model was designed for the electric current path computations. The concept of this model was motivated by the idea that electric currents are not flowing in full plasma volumes, but in current filaments and current sheets. Clearly this model can be used also for a modelling of the 3-D magnetic field. In some respects this model is similar to that of Sakurai (1981, 1989), which was used for the force-free magnetic field calculation with non-constant α. Our model is simple and we think that it can be successfully applied mainly in cases with few localized currents. We believe that it is the case of eruptive processes.

Acknowledgements. I acknowledge the support from the grant 303404 of the Academy of Sciences of Czech Republic and the grant 205/94/1577 of the Grant Agency of the Czech Republic. I would like to thank the referee, Dr. P. Démoulin, for his careful reviewing and useful comments.

References

Alfvén H., 1977, Rev. Geophys. Space Phys. 15, 271
Alfvén H., and Carlqvist P., 1967, Sol. Phys. 1, 220
Démoulin P., Hénoux J.C., Priest E.R., and Mandrini C.H., 1996, A&A 308, 643
de La Beaujardière J.F, Canfield R.C., and Leka K.D., 1993, ApJ 411, 378
Forbes T.G. and Isenberg P.A., 1991, ApJ 373, 294
Hagyard M.J., 1988, Sol. Phys. 115, 107
Hofmann A., 1995, Proc. of JOSO, Benešov, Czech Republic
Kaastra J.S., 1985,'Solar Flares: an Electrodynamic Model', Thesis, University of Utrecht, Utrecht
Klimchuk J.A., Lemen J.R., Feldman U., Tsuneta S., and Uchida Y., 1992, PASJ 44, L181
Kuperus M. and Raadu M.A., 1974, A&A 31, 189
Martens P.C.H., 1986, Sol. Phys. 107, 95
Melrose D.B., 1995, ApJ 451, 391
Priest E.R., 1994, in: Plasma Astrophysics, eds. J.G. Kirk, D.B. Melrore, E.R. Priest, Springer-Verlag, Berlin
Sakurai T., 1981, Sol. Phys. 69, 343
Sakurai T., 1989, Space Sci. Rev. 51, 11
Spicer D.S., 1982, Space Sci. Rev. 31, 351
Tajima T., Sakai J., Nakajima H. et al., 1987, ApJ 321, 1031
Van Tend W. and Kuperus M., 1978, Solar Phys. 59, 115

This article was processed by the author using Springer-Verlag LaTeX A&A style file *L-AA* version 3.